Minh Quang Pham
Ho Chi Minh City University of Technology (HCMUT)
Vietnam National University Ho Chi Minh City (VNU-HCM)
Vietnam

Thang Viet Vu
Ho Chi Minh City University of Technology (HCMUT)
Vietnam National University Ho Chi Minh City (VNU-HCM)
Vietnam

Lam Quang Tran
Ho Chi Minh City University of Technology (HCMUT)
Vietnam National University Ho Chi Minh City (VNU-HCM)
Vietnam

Huong Huu Nguyen
Nguyen Tat Thanh University
Vietnam

Thong Duc Hong
Ho Chi Minh City University of Technology (HCMUT)
Vietnam National University Ho Chi Minh City (VNU-HCM)
Vietnam

Study on Kinetics and Dynamics of the Scraping-pressing Mechanism of the Compactor Garbage Truck

This study comprehensively analyzed the kinematics and dynamics of the scraping-pressing mechanism of a garbage truck by using numerical methods. A multibody integrated with a hydraulic simulation model was established to investigate the mechanism's operation according to actual working conditions in a completed cycle with 18 seconds. The model was verified with the calculation at steady times, which showed high consistency. The results reveal that the mechanism operates in steady states almost all the time, with cylinder velocities ranging from 0.08 to 0.15 m/s. The cylinder velocity and acceleration fluctuate strongly when the mechanism accelerates or decelerates; however, the inertia effect is insignificant. The forces applied on joints are maximum at the end of the pressing process. Remarkably, the force applied on the joint connecting the scraping and sliding plate is highest, three times higher than the joint between the sliding plate and pressing cylinder and one and a half times higher than that between the scraping plate and scraping cylinder. The study's results can be applied to the design process of garbage trucks in special and specialized vehicles in general or used as a reference for enhancing the performance and optimizing the mechanism's mass, force, and materials.

Keywords: *Garbage truck, Scraping-pressing mechanism, Hydraulic system, Kinematics, Dynamics, Matlab Simscape.*

1. INTRODUCTION

Garbage trucks are an essential part of modern life, responsible for collecting and transporting garbage from our homes and businesses to processing or disposal facilities. The demand for garbage trucks in residential areas rises rapidly due to the enormous amount of garbage, with various types produced daily [1–3]. In particular, garbage compactor trucks with garbage compressing mechanisms are the most popular because they can carry large amounts of garbage.

While the compactor garbage trucks might seem simple at first glance, these trucks are complex machines, often incorporating hydraulic systems, compaction mechanisms, and various loading systems to handle different types of garbage. Designing an effective hydraulic-mechanical mechanism to satisfy the practical requirements of trucks is crucial. Thus, many studies were conducted to investigate and optimize the hydraulic-mechanical mechanisms of these garbage trucks. Zubov et al. [4] analyzed vehicle frame-free oscillations of a garbage truck with side mechanized loading. A new prototype of the grip was proposed to reduce the stresses and moments that appear in grip-container joints. Wang et al. [5] built a virtual prototype model of hydraulic-mechanical to evaluate the dynamics of the lifting mechanism on a garbage truck. The position of the revolute joint was optimized to reduce the lifting force of the cylinder. Shuping et al. [6] optimized the construction of the garbage collection mechanism for the garbage compactor to reduce the stress on the mechanism. Topology optimization was used on the multibody dynamics model to optimize the mass and strength of the lever arm. Fei et al. [7] designed and simulated the hydraulic system of the lifting mechanism on the Chengliwei garbage truck. The pressure, flow, velocity, and acceleration were analyzed to verify the correctness of the design scheme. Voicu et al. [8] examined the dynamics of the garbage compactor mechanism on a garbage compactor. The study's results provide additional insights into the mechanism's operation. Then, they analyzed the structure of the garbage compactor mechanism on a garbage compactor [9]. The strength of the press plate was tested under working conditions.

In addition, numerical simulation tools are increasingly used in research and design. They bring several conveniences in analyzing the kinematics and dynamics of hydraulic-mechanical structures [10–23]. Typically, Yihong et al. [10] used AMEsim software to analyze the velocity and acceleration of hydraulic cylinders for the lifting mechanism of small garbage trucks. The simulation results were verified by the experiment, showing high consistency. Xu et al. [11] analyzed the operation of the rear garbage collection mechanism of a garbage truck using ADAMS software. Through the evaluation results, the author proposed some improvements to the mechanism. Hong et al. [12] used 3D design software to model

Received: September 2024, Accepted: October 2024
Correspondence to: Thong Duc Hong, Ho Chi Minh City University of Technology Ly Thuong Kiet Street 268, District 10, Ho Chi Minh City, Vietnam
E-mail: hongducthong@hcmut.edu.vn
doi: 10.5937/fme2404603Q

two automatic releasing mechanisms on dump trucks. The mechanisms' kinematics and dynamics were then analyzed to show the advantages and disadvantages of each option. Luo et al. [13] investigated the dynamics of the garbage collection mechanism using ADAMS soft–ware. Based on the simulation results, genetic optimiza–tion was applied to optimize the mass of the mechanism. Hong et al. [14] used Matlab Simscape to model and compare the kinematics and dynamics of two opposing lifting mechanism arrangements on a dump truck.

The garbage truck has many mechanic-hydraulic mechanisms, such as the container lifting mechanism, garbage unloading mechanism, garbage loading mecha–nism, and scraping-pressing mechanism. The scraping-pressing mechanism is crucial in maximizing the effi–ciency and capacity of modern garbage trucks. This specialized mechanism is typically integrated into the rear of the garbage truck's container and employs a two-step process to compact the collected garbage. Firstly, a powerful hydraulic cylinder actuates the scraping plate to sweep the garbage inside the pre-compressor, initi–ating compaction. Subsequently, sliding and scraping plates are pulled to press the garbage into the garbage container. This coordinated action of pressing and scraping reduces the volume of the garbage, allowing the truck to accom–modate a larger payload before requiring unloading; it not only optimizes the collection process and minimizes the frequency of trips to landfills or processing plants, ulti–mately reducing operational costs and environmental im–pact. Although this mechanism is popular and practical, the studies focusing on its kine–matics and dynamics were minimal. Therefore, analyzing the kinematics and dynamics of the scraping-pressing mechanism is nece–ssary to provide the basis for designing or improving it in particular or specialized trucks.

In this study, a comprehensive simulation model of the scraping-pressing mechanism was established using Matlab Simscape. The multibody and hydraulic models were constructed using the Simmechanic and Simhyd–raulic modules. The accuracy of the simulation model was verified by comparing it with theoretical calculations. Then, the mechanism's kinematics and dynamics were investigated under operating conditions close to reality. This study aims to comprehensively analyze the kinematics and dynamics of the scraping-pressing mechanism under actual working conditions. From there, the study's results can be applied in the design of garbage compactor trucks in particular or specialized vehicles, in general to be able to design improvements, optimize dynamic features, optimize mass or materials, or improve the efficiency of the hydraulic system.

2. STRUCTURE OF THE SCRAPING-PRESSING MECHANISM

The mechanism is used on the popular Hino 300 series garbage truck. The garbage container has a volume of 8 m^3, and the maximum garbage load is 4080 kg. Figure 1a shows the structure of the garbage scraping-pressing mechanism. The mechanism includes a pre-compressor, a scraping plate, a sliding plate, two pressing cylinders, and two scraping cylinders. The sliding plate is placed on the two sliding tracks of the pre-compressor and can be mo–ved up and down by two pressing cylinders. The scraping plate is mounted on the sliding plate and can rotate with a maximum angle of 129 degrees by two scraping cylin–ders. Figure 1b shows the hydraulic circuit diagram used for the mechanism. The hydraulic circuit includes a hyd–raulic pump (1) that is powered by the engine, a direc–tional valve (3) used to control the movement direction of cylinders, and two sequence valves (4) and (5) used to control the operating order of the scraping cylinders (6a), (6b), and pressing cylinders (7a), (7b). The specifications of the pump and cylinders are shown in Table 1.

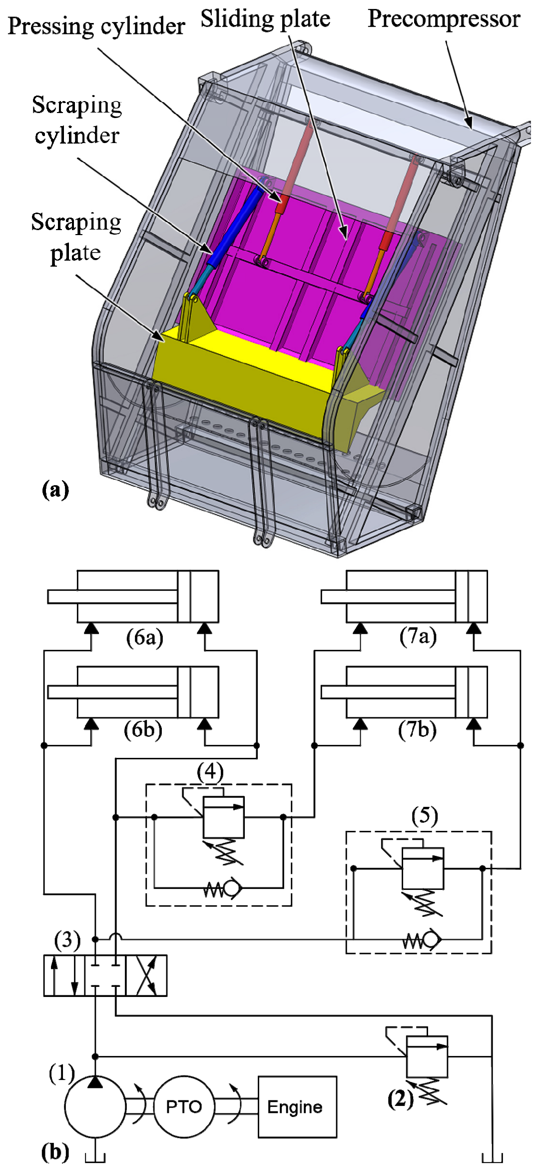

Figure 1. Construction of scraping-pressing mechanism: (a) 3D model, and (b) Hydraulic circuit diagram.

Table 1. Specifications of the hydraulic system.

Component	Specification	Value
Hydraulic Pump	Type	Fixed displacement
	Displacement	56 cc/rev
	Operating Speed	1000 rpm
	Working Pressure	250 bar
Scraping cylinder	Type	Double-Acting
	Displacement	0.5 m
	Cylinder diameter	0.08 m
	Piston rod diameter	0.05 m

Pressing cylinder	Type	Double-Acting
	Displacement	0.4 m
	Cylinder diameter	0.08 m
	Piston rod diameter	0.05 m

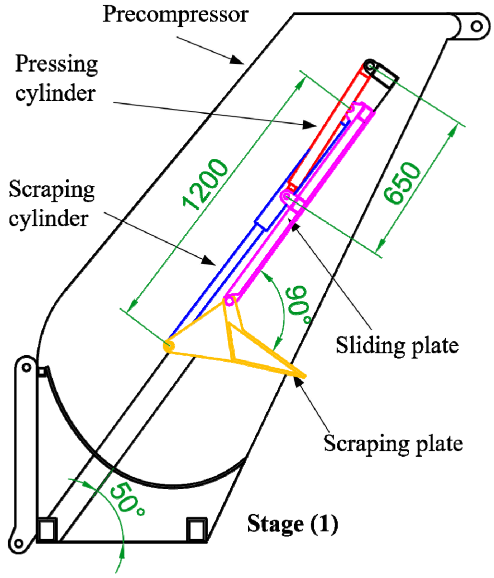

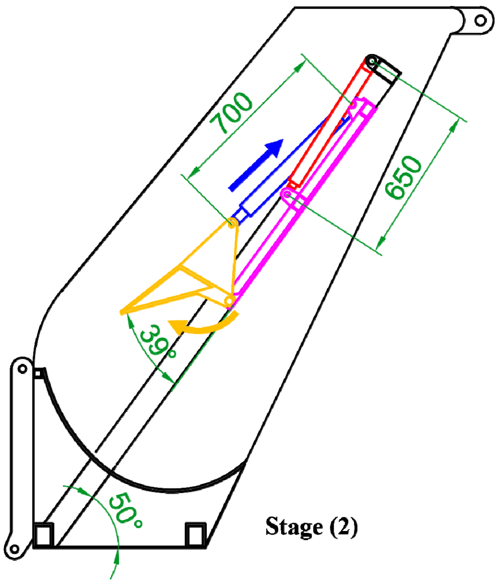

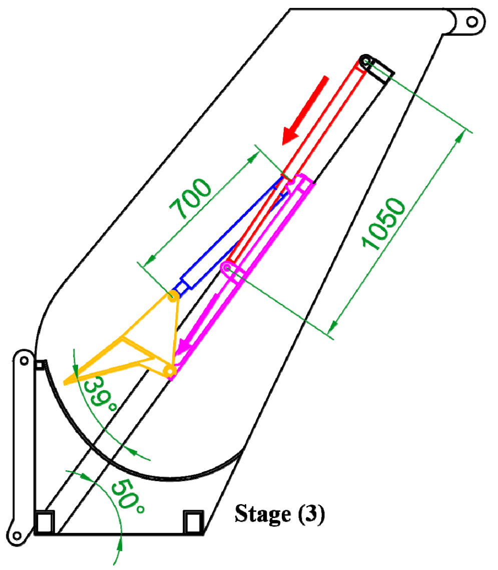

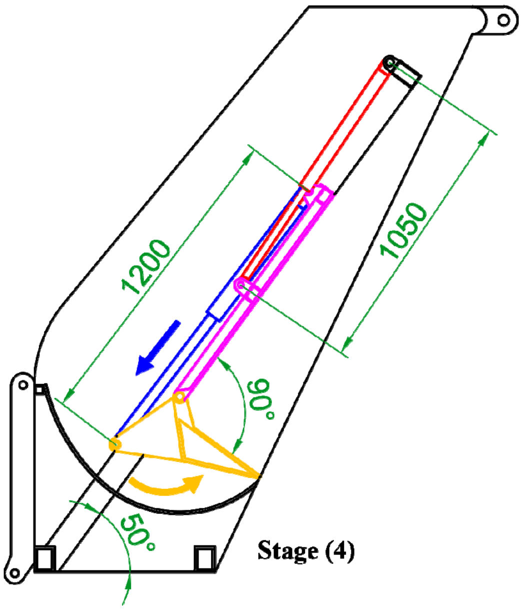

Figure 2. Operating process of the scraping-pressing mechanism.

Figure 2 shows the operating process of the scraping-pressing mechanism. The operating process of the mechanism consists of 2 processes formed from 4 operating stages: the preparation process and the scra–ping-pressing process. Stage (1) is the initial state; the mechanism is at the highest stage, and the scraping plate is closed, the pressing cylinder fully retracted, and the scraping cylinder fully extended; stage (2), the mechanism is still at the highest stage, and the scraping plate is opened, pressing and scraping cylinders fully retracted; stage (3) the mechanism goes down to the lowest stage, pressing cylinder fully extended and scra–ping cylinder fully retracted; stage (4) the mechanism is at the lowest stage and the scraping plate is closed. In the preparation process, the mechanism transforms from stage (1) to stage (2), then from stage (2) to stage (3) to approach the garbage in the pre-compressor. In the scraping-pressing process, the mechanism moves from stage (3) to stage (4) to rake the garbage inside the pre-compressor into the garbage container (scraping pro–cess), then from (4) to (1) to press all the garbage into the garbage container (pressing process). Thus, in the preparation process, the mechanism only bears the force of the mechanism's gravity. In the scraping-pressing process, the mechanism bears the loads when scraping and pressing garbage into the container.

3. BASIC FOR CALCULATING KINEMATIC AND DYNAMIC OF MECHANISM

Figure 3 presents the kinematic diagram of the scraping-pressing mechanism.

To analyze the kinematic of the mechanism, two vector loops are established:

$$\overrightarrow{AB}-\overrightarrow{AO}-\overrightarrow{OD}-\overrightarrow{DC}-\overrightarrow{CB}=0 \quad (1)$$

$$\overrightarrow{AB}-\overrightarrow{AO}-\overrightarrow{OD}-\overrightarrow{DF}-\overrightarrow{FG}-\overrightarrow{GE}-\overrightarrow{EC}-\overrightarrow{CB}=0 \quad (2)$$

Project these vector loops into the xOy coordinate:

$$L_{AB}\cos\varphi_1 - L_{OD} - L_{DC} = 0 \tag{3}$$

$$-L_{AB}\sin\varphi_1 + L_{AO} - L_{CB} = 0 \tag{4}$$

$$\begin{gathered} L_{AB}\cos\varphi_1 - L_{OD} - L_{FG}\cos\varphi_2 \\ + L_{GE}\cos\varphi_3 + L_{EC} = 0 \end{gathered} \tag{5}$$

$$\begin{gathered} -L_{AB}\sin\varphi_1 - L_{FG}\sin\varphi_2 + L_{GE}\sin\varphi_3 \\ + L_{AO} + L_{CB} - L_{DF} = 0 \end{gathered} \tag{6}$$

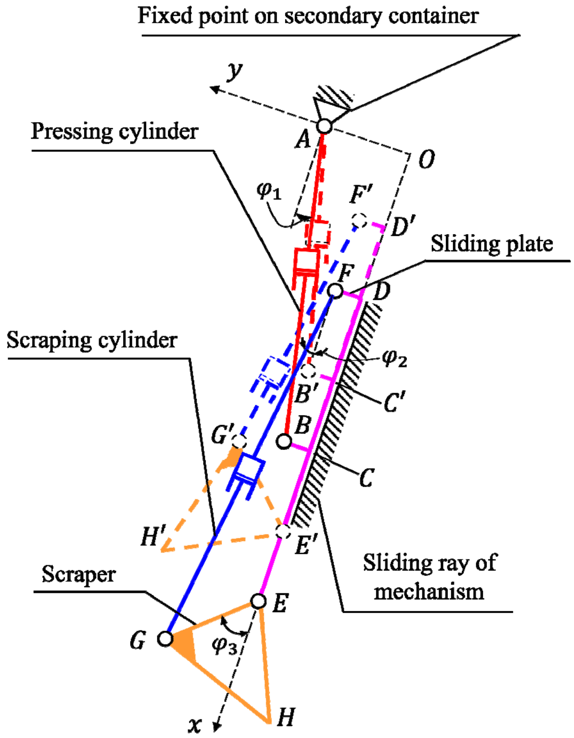

Figure 3. Kinematic scheme of the scraping-pressing mechanism.

where L_{AB}, L_{OD}, L_{DC}, L_{AO}, L_{CB}, L_{FG}, L_{GE}, L_{EC}, and L_{DF} are the distances from A to B, O to D, C to D, A to O, C to B, F to G, G to E, E to C, and D to F, respectively. L_{DC} = 0.455 m, L_{AO} = 0.105 m, L_{CB} = 0.065 m, L_{EC} = 0.495 m, L_{DF} = 0.065 m are the constant of the mechanism, L_{AB} and L_{FG} represent the length of the pressing cylinder and scraping cylinder, respectively. L_{OD} indicates the position of the sliding plate. φ_1, φ_2, and φ_3 are the angles between L_{AB}, L_{FG}, and L_{GE} and x-axis, respectively.

Differentiate time in Eqs. (3) to (6) to obtain the translational and angular velocity of the links.

$$\dot{L}_{AB}\cos\varphi_1 - \omega_1 L_{AB}\sin\varphi_1 - \dot{L}_{OD} = 0 \tag{7}$$

$$-\dot{L}_{AB}\sin\varphi_1 - \omega_1 L_{AB}\cos\varphi_1 = 0 \tag{8}$$

$$\begin{gathered} \dot{L}_{AB}\cos\varphi_1 - \omega_1 L_{AB}\sin\varphi_1 - \dot{L}_{OD} - \dot{L}_{FG}\cos\varphi_2 \\ + \omega_2 L_{FG}\sin\varphi_2 - \omega_3 L_{GE}\sin\varphi_3 = 0 \end{gathered} \tag{9}$$

$$\begin{gathered} -\dot{L}_{AB}\sin\varphi_1 - \omega_1 L_{AB}\cos\varphi_1 - \dot{L}_{FG}\sin\varphi_2 \\ - \omega_2 L_{FG}\cos\varphi_2 + \omega_3 L_{GE}\cos\varphi_3 = 0 \end{gathered} \tag{10}$$

where ω_1, ω_2, and ω_3 are the angular velocity of link AB (pressing cylinder), link FG (scraping cylinder), and link GEH (scraping plate), respectively. $\dot{L}_{AB}$, $\dot{L}_{OD}$ and $\dot{L}_{FG}$ are the translational velocities of the pressing cylinder, scraping cylinder, and sliding plate, respectively.

Finally, differentiate time in Eqs. (7) to (10) to obtain the angular and translational acceleration of links

$$\begin{gathered} \ddot{L}_{AB}\cos\varphi_1 - 2\omega_1\dot{L}_{AB}\sin\varphi_1 - {\omega_1}^2 L_{AB}\cos\varphi_1 \\ - \alpha_1 L_{AB}\sin\varphi_1 - \ddot{L}_{OD} = 0 \end{gathered} \tag{11}$$

$$\begin{gathered} -\ddot{L}_{AB}\sin\varphi_1 - 2\omega_1\dot{L}_{AB}\cos\varphi_1 \\ + {\omega_1}^2 L_{AB}\sin\varphi_1 - \alpha_1 L_{AB}\cos\varphi_1 = 0 \end{gathered} \tag{12}$$

$$\begin{gathered} \ddot{L}_{AB}\cos\varphi_1 - 2\omega_1\dot{L}_{AB}\sin\varphi_1 - {\omega_1}^2 L_{AB}\cos\varphi_1 \\ - \alpha_1 L_{AB}\sin\varphi_1 - \ddot{L}_{OD} - \ddot{L}_{FG}\cos\varphi_2 \\ - 2\omega_2\dot{L}_{FG}\sin\varphi_2 - {\omega_2}^2 L_{FG}\cos\varphi_2 - \alpha_2 L_{FG}\sin\varphi_2 \\ - {\omega_3}^2 L_{GE}\cos\varphi_3 - \alpha_3 L_{GE}\sin\varphi_3 = 0 \end{gathered} \tag{13}$$

$$\begin{gathered} -\ddot{L}_{AB}\sin\varphi_1 - 2\omega_1\dot{L}_{AB}\cos\varphi_1 + {\omega_1}^2 L_{AB}\sin\varphi_1 \\ - \alpha_1 L_{AB}\cos\varphi_1 - \ddot{L}_{OD} - \ddot{L}_{FG}\sin\varphi_2 \\ - 2\omega_2\dot{L}_{FG}\cos\varphi_2 + {\omega_2}^2 L_{FG}\sin\varphi_2 \\ - \alpha_2 L_{FG}\cos\varphi_2 - {\omega_3}^2 L_{GE}\sin\varphi_3 \\ + \alpha_3 L_{GE}\cos\varphi_3 = 0 \end{gathered} \tag{14}$$

where α_1, α_2, and α_3 are the angular acceleration of the pressing cylinder, scraping cylinder, and scraping plate, respectively. $\ddot{L}_{AB}$, $\ddot{L}_{OD}$ and $\ddot{L}_{FG}$ are the translational acceleration of the pressing cylinder, scraping cylinder, and sliding plate, respectively.

The force diagram of the scraping-pressing mechanism is indicated in Figure 4.

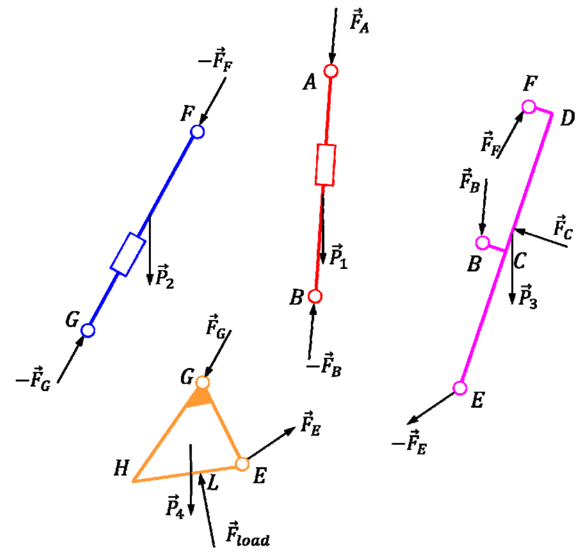

Figure 4. Froce diagram of the scraping-pressing mechanism.

Considering the link AB:

$$\vec{F}_A - \vec{F}_B + \vec{P}_1 = M_1\vec{a}_{m1} \tag{15}$$

$$\vec{r}_{Am1} \times \vec{F}_A - \vec{r}_{Bm1} \times \vec{F}_B = I_{1m}\alpha_1 \tag{16}$$

where M_1 is the mass of the pressing cylinder $\vec{F}_A$, $\vec{F}_B$ and $\vec{P}_1$ are the force applied on joins A, B and the gra–

vitational force of link AB. $\vec{a}_{m1}$ is the acceleration of link AB's mass center. $\vec{r}_{Am1}$ and $\vec{r}_{Bm1}$ are the vectors from A, and B to the mass center. I_{1m} is the inertia mo–ment through the mass center.

Considering the link FG:

$$-\vec{F}_F - \vec{F}_G + \vec{P}_2 = M_2 \vec{a}_{m2} \tag{17}$$

$$-\vec{r}_{Fm2} \times \vec{F}_F - \vec{r}_{Gm2} \times \vec{F}_G = I_{2m} \alpha_2 \tag{18}$$

where M_2 is the mass of the pressing cylinder. $\vec{F}_G$ is the force applied on joins G. and $\vec{P}_2$ is the gravitational force of link FG. $\vec{a}_{m2}$ is the acceleration of link FG's mass center. $\vec{r}_{Fm2}$ and $\vec{r}_{Gm2}$ are the vector from F, G to the mass center. I_{2m} is the moment of inertia through the mass center.

Considering the link BCDEF:

$$\vec{F}_B - \vec{F}_E + \vec{F}_F + \vec{F}_C + \vec{P}_3 = M_3 \vec{a}_{m3} \tag{19}$$

$$\begin{aligned} &\vec{r}_{Bm3} \times \vec{F}_B - \vec{r}_{Em3} \times \vec{F}_E + \vec{r}_{Fm3} \\ &\times \vec{F}_F + \vec{r}_{Cm3} \times \vec{F}_C = I_{3m} \alpha_3 \end{aligned} \tag{20}$$

where M_3 is the mass of the pressing cylinder. $\vec{F}_E$, $\vec{F}_C$ is the force applied on joins E and C. $\vec{P}_3$ is the gravitational force of link BCDEF. $\vec{a}_{m3}$ is the acceleration at the link BCDEF's mass center. $\vec{r}_{Bm3}$, $\vec{r}_{Em3}$, $\vec{r}_{Fm3}$, and $\vec{r}_{Cm3}$ are the vector from B, E, E, F, and C to the mass center. I_{3m} is the moment of inertia through the mass center.

Considering the link EGH:

$$\vec{F}_E + \vec{F}_G + \vec{F}_{load} + \vec{P}_4 = M_4 \vec{a}_{m4} \tag{21}$$

$$\begin{aligned} &\vec{r}_{Em4} \times \vec{F}_E + \vec{r}_{Gm4} \times \vec{F}_G \\ &+ \vec{r}_{Lm4} \times \vec{F}_{load} = I_{4m} \alpha_4 \end{aligned} \tag{22}$$

where M_4 is the mass of the pressing cylinder. $\vec{P}_4$ is the gravitational force of link EGH. $\vec{a}_{m4}$ is the acceleration at the link EGH's mass center. $\vec{r}_{Em4}$, $\vec{r}_{Gm4}$, and $\vec{r}_{Lm4}$ are the vectors from E, G, and L to the mass center. I_{4m} is the moment of inertia through the mass center. $\vec{F}_{load}$ is the garbage load applied on the scraping plate.

4. BASIC OF HYDRAULIC SYSTEM

The flow rate of the fixed displacement hydraulic pump:

$$Q_p = Dn - C \Delta p_p \tag{23}$$

where Q_p, D, n, C, and Δp_p are the pump flow rate, pump displacement, pump speed, leakage coefficient, and the pressure gain of the pump.

The flow rate of oil goes into the cylinder chamber:

$$Q_c = \frac{d\left(\dfrac{\rho V}{\rho_o}\right)}{dt} \tag{24}$$

where Q_c is the cylinder flow rate, V is cylinder volume, ρ_o and ρ is the hydraulic oil density at atmosphere pressure and hydraulic oil density in the cylinder.

The force generated by the cylinder:

$$F_c = p_A S_A - p_B S_B \tag{25}$$

where F_c is the cylinder force, p_A and p_B are the pressure in sides A (extend side) and B (retract side) of the cylinder, respectively, S_A and S_B are the pressure in sides A and B of the cylinder, respectively.

Hard stop force of cylinder.

$$F_{stop} = \begin{cases} K\left(x - D_n\right) + Bv \text{ for } x \geq \mathrm{D}_n \\ K\left(-x\right) + Bv \text{ for } x \leq 0 \end{cases} \tag{26}$$

where x is the position of the piston rod, D_n is the nominal displacement of the cylinder, K and B are the stiffness and damping coefficient of the cylinder hard stop, respectively. v is the cylinder velocity

5. SIMULATION MODEL

Mechanism multibody model

Figure 5 presents the Simscape multibody model of the scraping-pressing mechanism. The pre-compressor is the frame used to link other components. The sliding plate is linked with a pre-compressor by Prismatic-1 & Prismatic-2 joints. Two pressing cylinders and two pressing pistons are connected to the pre-compressor and sliding plate by Revolute-1, Revolute-2, Cylinderical-1, and Cylinderical-2 joints, respectively. The scraping plate and sliding plate are connected by Revolute-5 and Revolute-6 joints. Two scraping cylinders and two scraping pistons are connected to the sliding plate and scraping plate by Revolute-3, Revolute-4, Cylinderical-3, and Cylinderical-4 joints, respectively. Prismatic-3, Prismatic-4, Prismatic-5, and Prismatic-6 joints are utilized to link between cylinders and pistons; they are connected to the hydraulic model to describe the cylinder operations. The garbage load is applied to the center point of the scraping plate surface and varies according to the mechanism's operating process.

Simulation hydraulic model

Figure 6 presents the simulation hydraulic model of the scraping-pressing mechanism, which is constructed according to the hydraulic circuit diagram in Figure 1b. The directional valve is controlled by a physic signal to change the direction of movement of hydraulic cylinders. The simulation process is performed in 18 secon–ds: during 0-8.3s, the valve is in a positive position; then, during 8.5-18s, the valve is in a negative position. The valve reserval time is set to 0.2s. The hydraulic pump operates at a speed of n = 1000 rpm. The relief valve pres–sure at pump output is set to 250 bar. The opening pressure of sequence valves is set to 100 bar. The opening pressure of the check valve in the sequence valves is 5 bar to avoid the mechanism falling down when no load is applied.

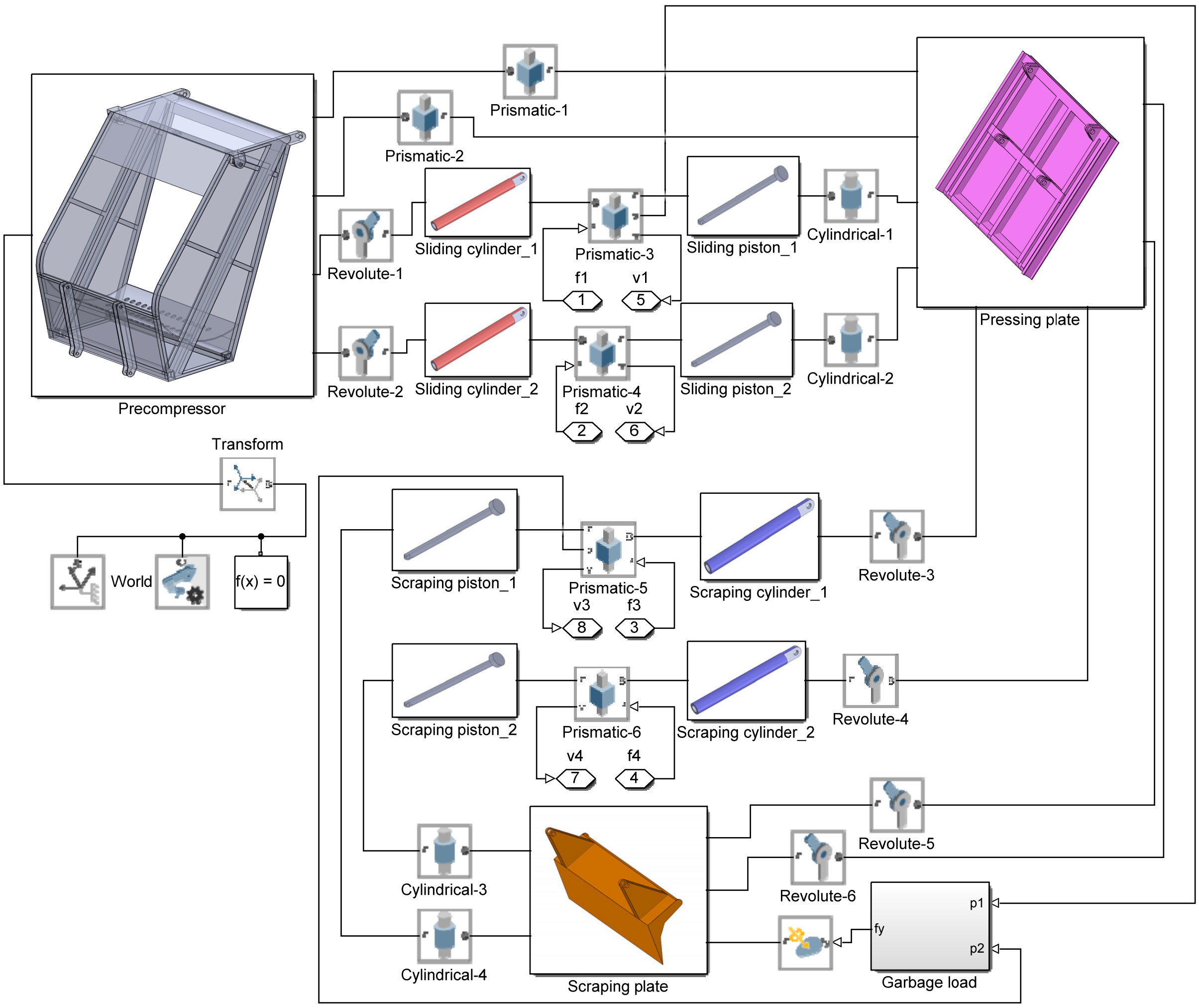

Figure 5. Simscape multibody model of the scraping-pressing mechanism.

Garbage load

The garbage load acting on the mechanism is considered when operating in the final cycles to press the garbage into the container. At this time, the mechanism will need to create the largest pressing force to push the garbage from the pre-compressor into the garbage container because the container is full of garbage. Assuming that the garbage has filled the entire volume of the pre-compressor during the scraping process, the garbage load is the frictional force between the garbage and the pre-compressor walls. Then, during the pressing process, the garbage load is the frictional force between all the garbage in the container and the container walls. Based on the experience of design engineers in practice, the coefficient of friction between the garbage and the container can reach a maximum of 1. Thus, the garbage load acting on the mechanism is calculated according to figure 6.

Garbage load during the scraping process:

$$F_{load\_1} = V_{sc}\rho_g f = 300 \text{ (kg)}$$

where V_{sc} = 1 m^3 is the maximum garbage volume in the secondary container, ρ_g = 300 kg/m^3 is the garbage density, f = 1 is the friction coefficient between garbage and container.

Garbage load during the pressing process:

$$F_{load\_2} = \frac{V_{pc}\gamma\rho_g f}{\sin\beta} = 6550 \text{ (kg)}$$

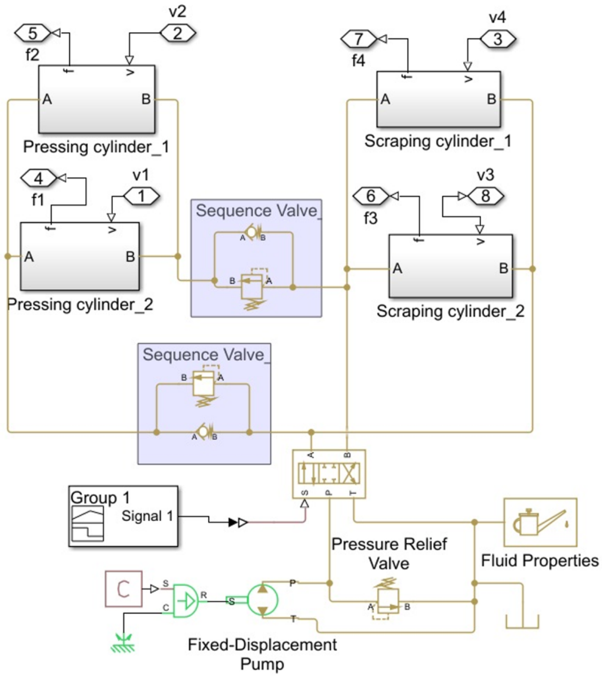

Figure 6. Simscape hydraulic model of the scraping-pressing mechanism.

where V_{pc} = 8 m^3 is the garbage volume in the primary container, γ = 1.7 is the compression ratio, β is the angle between the scarping plate surface and the primary container bottom.

Figure 7 presents the garbage load acting on the mec–hanism: (a) the illustration of the applied force model, and (b) the variation of garbage load according to time during the simulation process. The garbage load is placed at the center of the scraper and is always perpendicular to the scraper surface. In practice, when pressing, the garbage load increases gradually from the start of pressing until the garbage is pushed into the container, so the garbage load is assumed to increase from the start of pressing until the edge of the scraper reaches the floor position of the main bin (within the height h).

In the first 8.5s (Preparation process), the garbage force acting on the mechanism is 0. From 8.5s to 13.92s, the force generated by the garbage in the pre-compressor, F_{load_1}. From 13.92s to 15.1s, the garbage force increases gradually from F_{load_1} to F_{load_2}, corresponding to the time the mechanism moves up to the garbage container's floor. After 15.1 seconds, the garbage force is F_{load_2}.

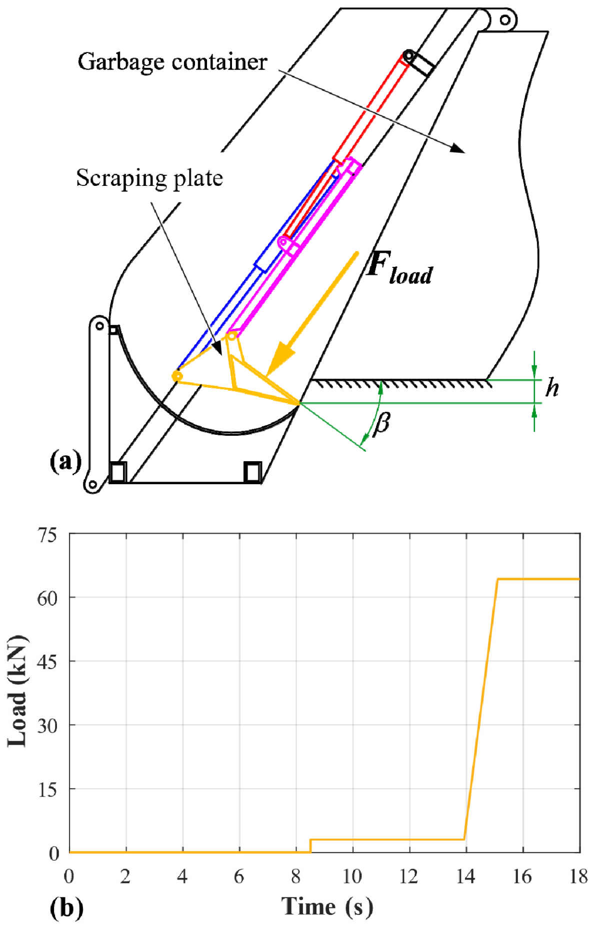

Figure 7. The garbage load acting on the mechanism: (a) the illustration of the applied force model, and (b) the variation of garbage load according to time during the simulation process.

6. RESULTS AND DISCUSSIONS

6.1 Cylinders' displacement, velocity and acceleration

Figure 8 reveals the variation in scraping and pressing cylinders' displacement, velocity, and acceleration. At the beginning of the simulation, the scraping cylinder reduces its displacement from 0.5 m to 0 m with a constant velocity of –0.15 m/s, while the pressing cylinder is stationary, in times t = 0 – 3.27s. Then, as t = 3.27 – 8.3s, the scraping piston is stationary, and the pressing piston increases its displacement from 0 to 0.4 m with a velocity of 0.08 m/s. During t = 8.3 – 8.5s, the directional valve changes position, leading to pressure changes in the cylinder chambers, causing the pistons to have strong fluctuations in acceleration and velocity. Next, the scraping piston is extended from 0 – 0.5m at a velocity of about 0.0925 m/s, while the pressing piston remains stationary at the displacement of 0.4 m, in the time of t = 8.5 – 13.86s. Then, the scraping piston is stationary for the remainder of the cycle. The pressing piston starts moving when t > 13.86 with an initial velocity of about –0.12 m/s and gradually decreases to –0.1 m/s at t = 14.87s due to the increasing load of garbage during this period; then, the piston moves to the end of its stroke at t = 17.61s with a velocity of about 0.108 m/s.

The acceleration of the pistons oscillates vigorously during sudden acceleration and deceleration due to the piston interacting with the cylinder housing through the hard stop model and compressibility of the fluid. The maximum acceleration values of the scraping and pressing piston are 68 and 35 m/s^2, respectively. The influence of the hard stop model will be explained in more detail later.

In addition, after oscillation, the acceleration of the piston is almost zero due to the velocity being nearly constant. Although the cylinders' velocity and acceleration significantly fluctuate, the displacement remains stable throughout the simulation, showing that inertia's effect insignificantly impacts the stabilization of the mechanism's operation.

6.2 Cylinders' pressure and flowrate

The pressure and flow rate entering the scraping cylinder are presented in Figure 9. As shown in Figure 9a, at the beginning of the preparation process, the oil flow rate entering chamber B is about 27.56 Lpm, and the pressure is about 11.57 bar (t = 0 – 3.27s), making the scraping cylinder start to retract. Then, the oil pressure increases to 105 bar, which is higher than the sequence valve pressure, and the oil flow rate entering the cylinder also decreases to 0 (t = 3.27 – 8.3s). Considering Figure 9b, at the beginning of the scraping-pressing process, the oil enters chamber A of the cylinder with the oil flow rate of 27.75 Lpm, and the pressure increases from 6.06 to 9.49 bar (t = 8.5 – 13.82s), making the cylinder extend and scrap garbage.
After completing the stroke, the pressure in the chamber increases to 130 bar (t = 13.86) to open the sequence valve and continues to rise gradually to 225 bar (t = 15.1s) due to the increase in garbage load. Although the cylinder stroke is completed during t = 13.86 and 15.1s, the cylinder flow rate remained at 1.22 Lpm because the hard stop model caused the extra moving of the piston to balance between reaction force and pressure.

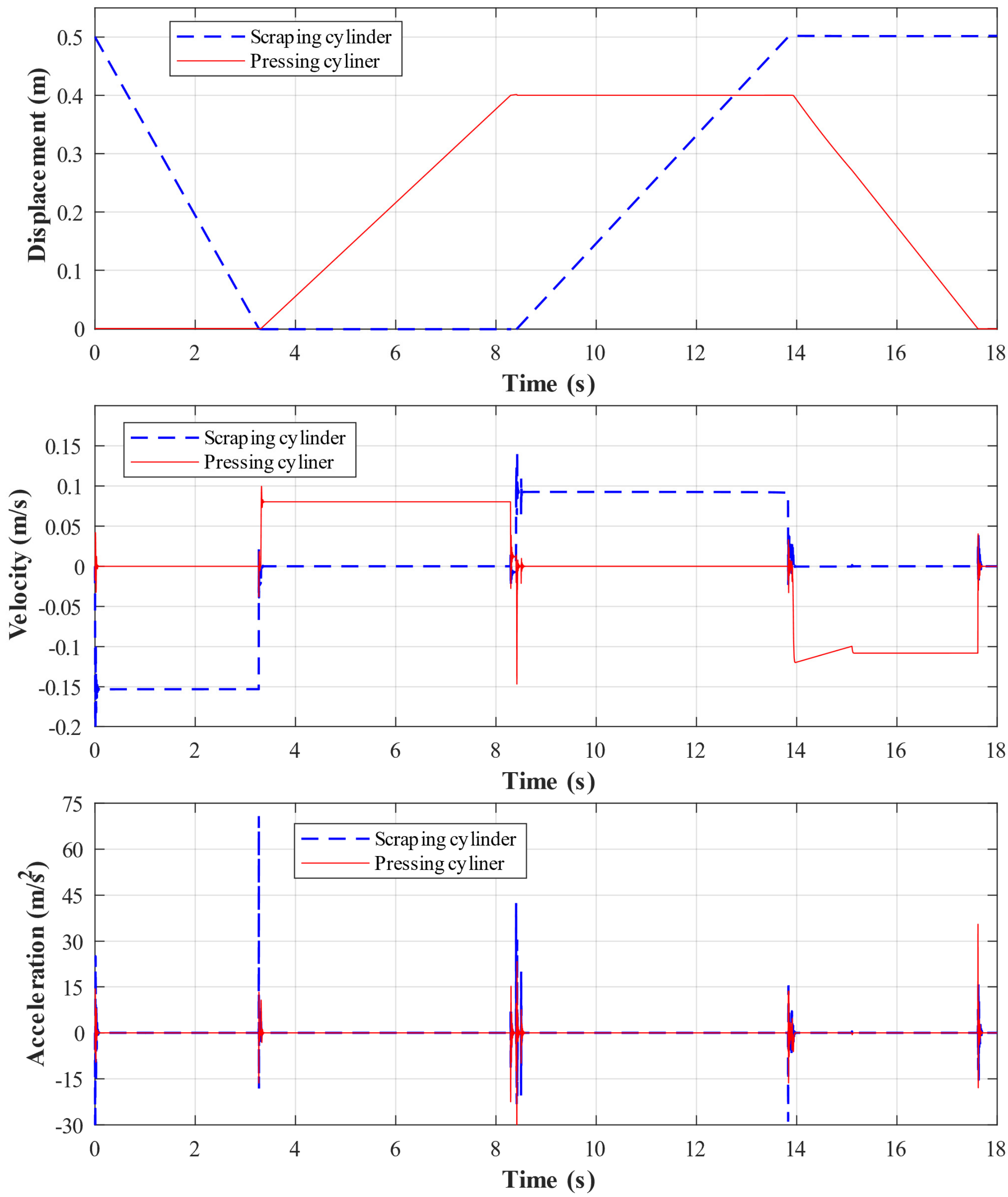

Figure 8. The variation in displacement, velocity, and acceleration of the scraping cylinder and pressing cylinder.

Similarly, at the end of stages 1 and 2, due to the sudden increase in pressure when the cylinder moves to the end of the stroke, the extra moving suddenly occurs, leading to instantaneous flow in the cylinder chambers. How–ever, these effects are only transient and do not signi–ficantly affect the overall operation of the mechanism.

Figure 10 shows the pressure and flow rate in the pressing cylinder. Considering Figure 10a, at the begin–ning of the preparation process, the pressing cylinder flow is 0 Lpm, and the pressure in the chamber is 0.07 bar (t = 0 – 3.27s). When the sequence valve is opened at 3.27s, the flow into chamber A of the cylinder is 24.1 Lpm, and the pressure is only 4.95 bar because the cylinder only needs to push the mechanism down without garbage load. Considering Figure 10b (scraping-pressing process), the pressing cylinder flow is also 0 at the beginning during t = 8.5 – 13.82s. When the sequence valve is opened, the oil flow immediately reaches 13.96 Lpm, and the pressure is 29.88 bar; then, the flow gradually decreases because the increasing pressure causes an increase in the leakage flow of the pump. Finally, at maximum garbage load, the pressure is 124.77 bar, and the flow rate is 19.65 Lpm. Similar to the scraping cylinder, the pressing cylinder flow rate also fluctuates when the pressure suddenly increases at the end of stages or when the sequence valve opens.

In addition, the flow rate of the pressing cylinder is always lower than that of the scraping cylinder because the pressure at the pump is always greater than or equal to the sequence valve pressure during the pressing cylinder operation, leading to a decrease in the pump flow rate. This result also explains why the speed of the pressing cylinder is always lower than that of the scra–ping cylinder.

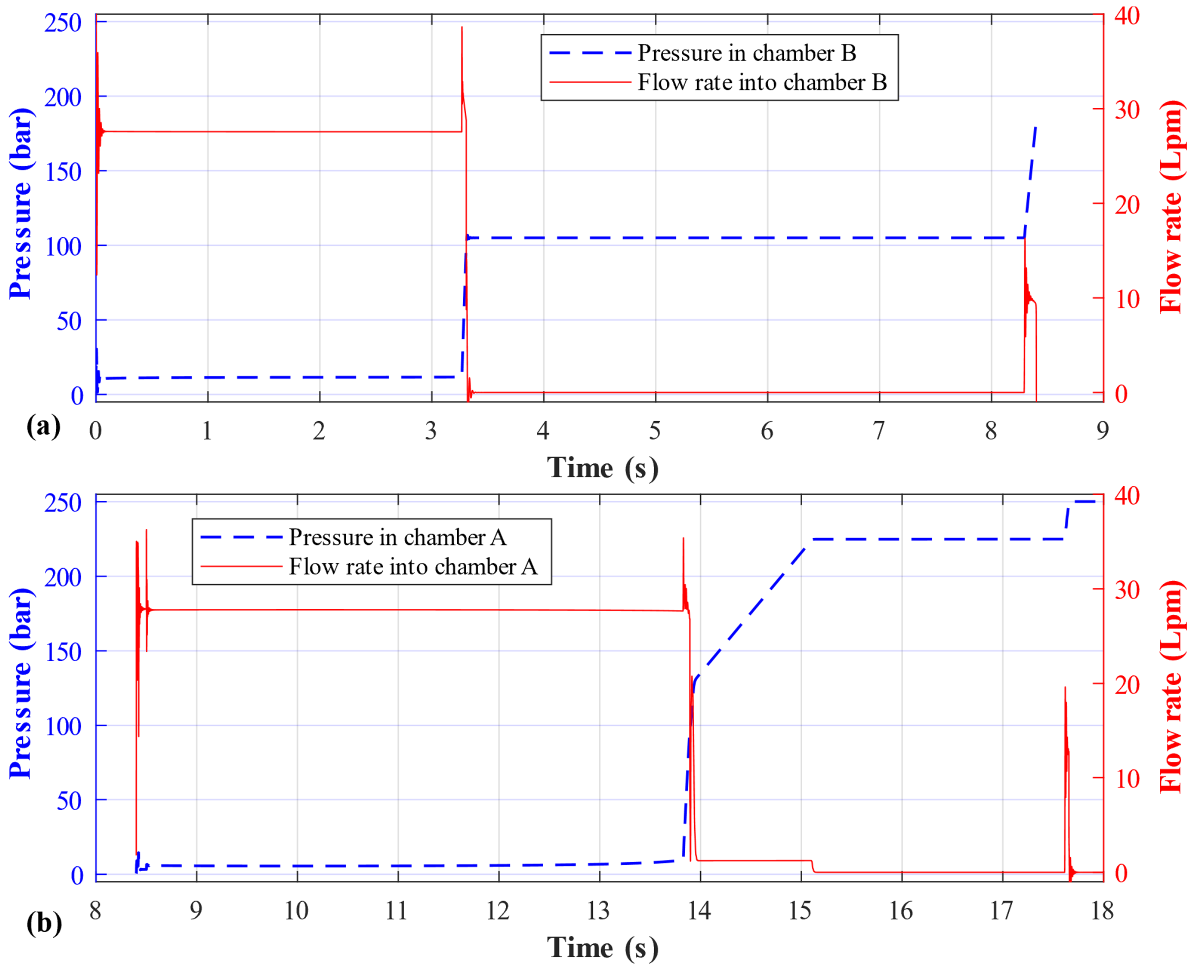

Figure 9. Pressure and flow rate of the scraping cylinder: (a) in chamber B of the preparation process, and (b) in chamber A of the scraping-pressing process.

6.3 Cylinders' forces

Figure 11 shows the forces generated by scraping and pressing cylinders obtained from simulation and calculation. Note that the positive direction is the direction of extension of the cylinders. Considering the variation of simulation forces during the steady-state processes, in the period t = 0 – 3.27s, the force of the scraping cylinder gradually decreases from –0.05 to –0.33 kN, which is the force required to balance the self-weight of the scraping plate; meanwhile, the force of the pressing cylinder is kept constant at – 1.01 kN, which is the necessary force to balance the self-weight of the entire mechanism. In the period t = 3.4 – 8.3s, the forces of the two cylinders are kept constant at – 0.33 and – 1.01 kN, respectively. Next, in the period t = 8.6 – 13.82s, the scraping cylinder force increases along a curve from 0.97 to 2.86 kN due to the scraping plate rotating and the garbage load acting perpendicular to it, while the pressing cylinder force decreases linearly from – 0.11 to –2.46 kN. Finally, after t = 13.86, the scraping cylinder force gradually increases with the load and reaches its maximum value of 62.22 kN. In contrast, the pressing cylinder force gradually decreases to the minimum value of –31.71 kN.

To ensure the accuracy of the simulation model, the authors calculated the cylinder force when the mechanism is in steady states (velocity is almost constant, acceleration is nearly zero) at t = 0.1s, t = 2s, t = 3.4s, t = 6s, t = 8.6s, t = 11s, t = 13.82, t = 14.5s, and t = 17.61s. The results show that the simulation results agree well with the calculation results. The magnitude values of the simulation result are always higher than the calculation because the calculation neglects the cylinder weight and the effect of inertia. The error between the two methods is lower than 5%.

6.4 Force at joints

Figure 12 reveals the magnitude values of (a) the force at joint G, the joint between the scraper cylinder and the scraper table (equal to the force at joint F); (b) the force at joint B, the joint between the press cylinder and the slide table (equal to the force at joint A); and (c) the force at joint E, the force at the joint between the scraping and sliding plate. Note that these forces are taken on one side of the mechanism since the mechanism is symmetrical about the vertical axis.

Considering the steady-state forces of the mechanism in the preparation process, the mechanism only bears its weight, so the forces at the joints are also small. At t = 0.1s, F_G is 0.05 kN, then it gradually increases to 0.33 kN at t = 3.27s. F_B is kept constant at 1.03 kN from t = 0.1 – 3.27s. F_E gradually decreases from 0.47 to 0.37 kN at t = 0.1 – 3.27s. Next, during t = 3.27 – 8.3s, F_G, F_B, and F_E are remained constant at 0.33, 1.015, and 0.37 kN values, respectively.

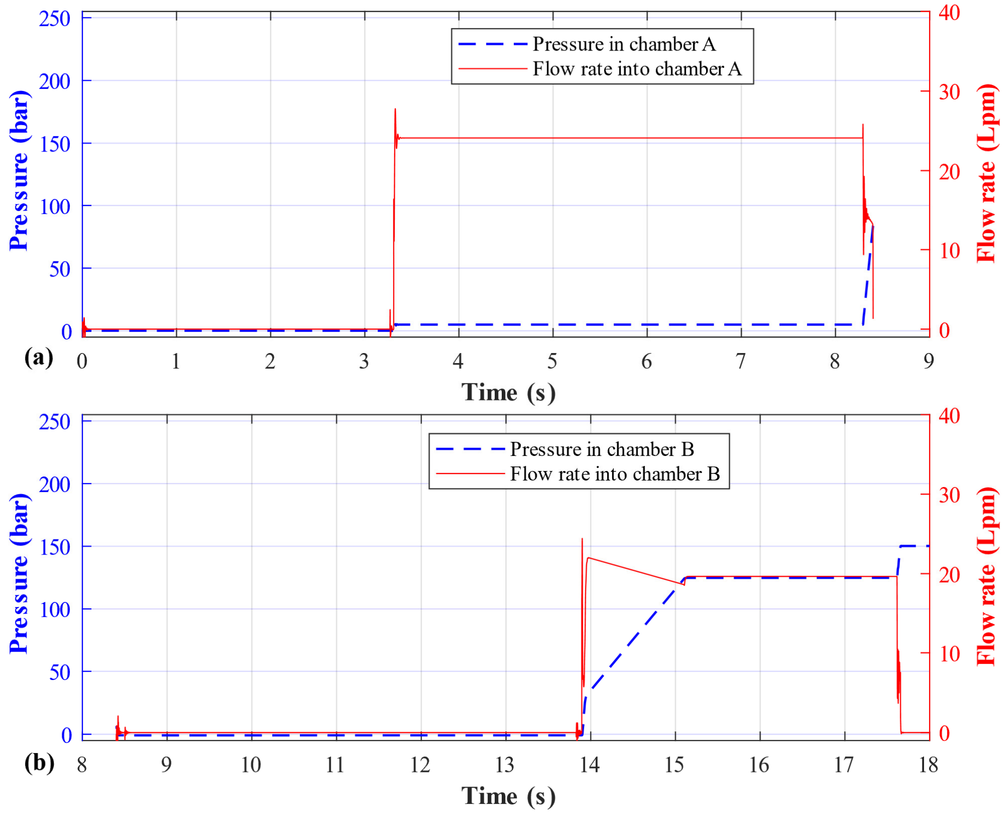

Figure 10. Pressure and flow rate of the pressing cylinder: (a) in chamber A of the preparation process, and (b) in chamber B of the scraping-pressing process.

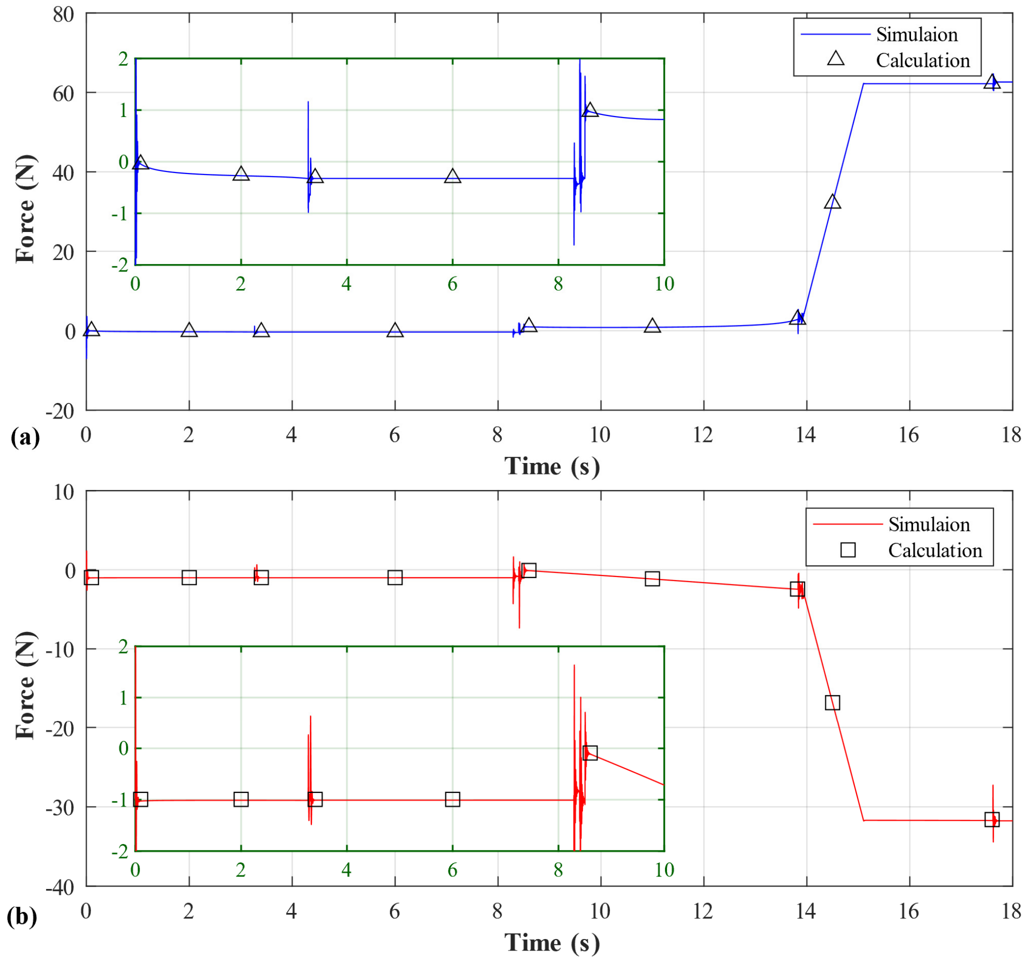

Figure 11. Calculation and simulation cylinder forces of (a) scraping cylinder, and (b) pressing cylinder.

Considering the steady-state forces of the mecha–nism in the scraping-pressing process, as t = 8.5 – 13.92s, F_G increases in a curve from 0.97 to 2.85 kN, F_B increases linearly from 0.118 to 2.47 kN, and F_E increases in a curve from 1.22 to 4.721 kN. While t = 13.92 – 15.1s, the forces at the joints increase linearly due to the increase in the load, and at t = 15.1s, F_G, F_B, and F_E reach their maximum values of 62.19, 31.71, and 94.01 kN, respectively, after which these forces remain constant until the end of the simulation.

Regarding the dynamics force, the pins experience instantaneous force because of the inertial forces when the cylinder accelerates or decelerates suddenly. Due to their impact, the maximum values of the forces F_G, F_B, and F_E are 64.59, 34.31, and 97.50 kN, respectively, which are higher than the steady values but not considerable in this mechanism case.

Besides, in the preparation process, F_B is always larger than F_G and F_E because the pressing cylinder must hold the entire mechanism. However, in the scraping-pressing process, when the garbage load is applied, F_G increases quickly because the lever arm of the scraping cylinder decreases sharply; therefore, F_G is finally twice as large as F_B. In addition, because joint E acts as a fulcrum for the scraping plate, the reaction force at this joint is the largest when pressing the garbage, nearly 3.1 times larger than F_B and 1.5 times larger than F_G.

This result can be used to analyze the strength of the pins when designing the mechanism. Furthermore, these results show that the structure strongly influences the force value acting on the pins. Therefore, optimizing the struc–ture is necessary to harmonize the forces acting on the pins, helping to design the mechanism more effectively.

7. CONCLUSIONS

In this study, the authors establish a mechanical-hydra–ulic simulation model of the scraping-pressing mecha–nism of the garbage truck. The kinematics and dynamics of the mechanism are analyzed in depth according to the actual operating conditions of the mechanism.

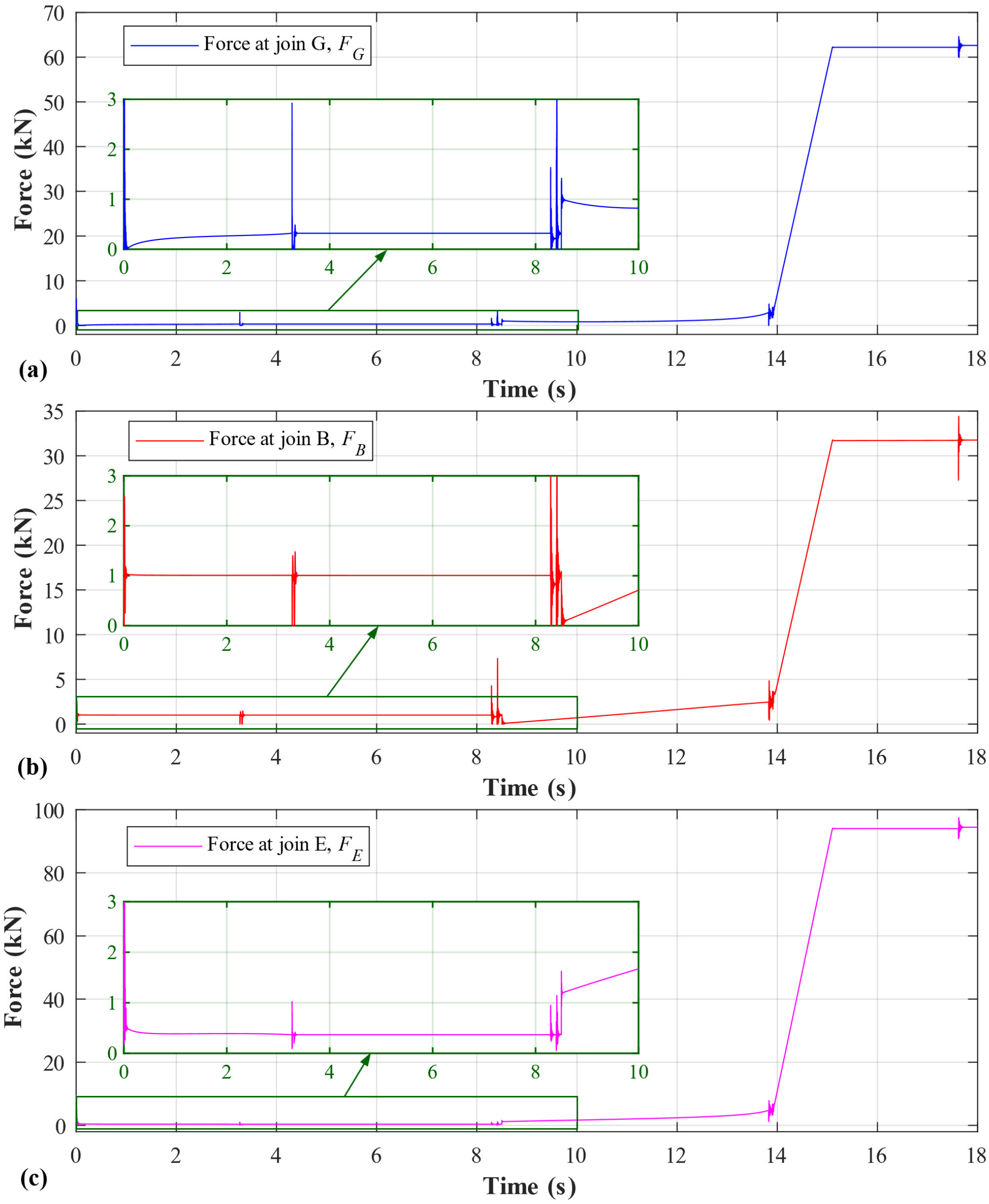

Figure 12. Forces at joints of the mechanism: (a) joint G, (b) joint B, and (c) joint E.

The model simulates the operation of the mechanism with a total operating time of about 18 seconds. At nearly all times, the mechanism operates in a steady state, with the operating speeds of the scraping and pressing cylinders being about 0.098 - 0.15 m/s and 0.08 - 0.12 m/s, respectively.

Regarding the forces applied on joints, all forces reach the maximum values at the end of the pressing process. At that time, the force applied on the joint between the scraping plate and cylinder is twice that of the joint between the sliding plate and the pressing cylinder, while the joint between the sliding and scraping plate bears the most significant force, three times higher than that of the joint between the sliding plate and the pressing cylinder.

Regarding dynamic loads acting on the mechanism, they are generated by the acceleration of the hydraulic cylinders from the start until stable speeds and vice versa, caused by the effect of the cylinder's damping and by the compression of the working fluid, which is considered in real-time. Although dynamic loads cause fluctuations in velocity, acceleration pressure, flow rate, and force, the influence of inertia on the scraping-pressing mechanism is inconsiderable.

The simulation results are highly consistent with calculations, with the force error of the cylinders at stable times less than 5%. The simulation results are always higher because they consider the whole mechanism weight and inertia force.

The proposed model can be applied in practice to accurately analyze and predict the kinematics and dynamics of the mechanism, with the dynamic forces considered, thereby bringing many conveniences and speeding up the design process. It is crucial in designing to determine the safety factor and lifespan of the components in the mechanisms when they bear fatigue due to dynamic forces. In addition, the study contributes a reference for optimizing the mechanism to improve operating efficiency, reduce mass and the forces acting on the mechanism, and investigate the effect of hydraulic component setup on the mechanism operation.

ACKNOWLEDGMENT

We acknowledge Ho Chi Minh City University of Technology (HCMUT), VNU-HCM for supporting this study.

REFERENCES

[1] Castillo B., H.: Garbage, work and society. Resour. Conserv. Recycl, Vol. 39, pp. 193–210, 2003.

[2] Olszowiec, P.: Garbage truck operation in an urban area, TransNav, Vol. 15, pp. 911–914, 2021.

[3] Qiang, S., Guoxiang, L., Shuzhan, B. and Chengcheng, M.: The simulation study of hybrid compression garbage trucks, Adv. Mat. Res, Vol. 608–609, pp. 1220–1224, 2013.

[4] Zubov, V. V., Domnitskiy, A. A. and Kargin, R. V. Calculation and choice of grip parameters for garbage truck manipulator, Procedia Eng, Vol. 129, pp. 896–902, 2015.

[5] Wang, Z., Liu, D., Jiang, R. and Ge, X.: Optimum design of kitchen garbage truck lifting mechanism based on virtual prototype, Adv. Mat. Res, Vol. 479–481, pp. 837–840, 2012.

[6] Shuping, Z., Zengjie, Y. and Lei, X.: Hydraulic System Design and Simulation of the Lifting Device for the Hanging Barrel Campus Garbage Truck, J. Phys. Conf. Ser, Vol. 2450, p. 012050, 2023.

[7] Fei, L., Qiao, X. and Zhang, S.: Hydraulic system design and simulation of the lifting device for the hanging barrel campus garbage truck, J. Phys. Conf. Ser, Vol. 2450, p. 012050, 2023.

[8] Voicu, G., Lazea, M., Zabava, B.-S., Tudor, P. and Moise, V.: Cinematical analysis of the pre-taking and pre-compacting mechanisms of some garbage trucks, J. Eng. Stu. Res, Vol. 25, pp. 56–62, 2019.

[9] Voicu, G., Lazea, M., Constantin, G. A., Stefan, E. M. and Munteanu, M. G.: Finite element analysis of the compaction plate from a garbage truck, E3S Web Conf., Vol. 180, p. 04006, 2020.

[10] Yihong, Z., Bo, J., Zhengkun, W. and Ran, D.: Dynamic Analysis of Hydraulic System of a Mobile Garbage Compression Equipment Based on AMESim, in: *Proc. 1st Int. Conf. Mech. Eng. Mater. Sci.*, 2012, Paris, pp. 54–56.

[11] Xu, W., Zhang, C. and Wang, S.: Design and simulating analysis of compressed garbage transport truck lifting mechanism based on ADAMS, Appl. Mech. Mater, Vol. 215–216, pp. 1224–1227, 2012.

[12] Hong, T. D., Nguyen, Y. T. H., Le, L. T., Pham, M. Q., Huynh, T. P. and Nguyen, T. T.: Comparative Study on Auto-Releasing Mechanisms of Tipper Truck, in: *Proc. - 2022 9th NAFOSTED Conference on Information and Computer Science*, 2022, Ho Chi Minh City, pp. 394–400.

[13] Luo, L., Li, X. and Yuan, M.: Lightweight Optimization of Garbage Collection Truck Manipulator Based on Parametric Modelling, J. Phys. Conf. Ser., Vol. 2587, p. 012032, 2023.

[14] Hong, T. D., Pham, M. Q., Tran, S. C., Tran, L. Q. and Nguyen, T. T.: A comparative study on kinetics and dynamics of two dump truck lifting mechanisms using MATLAB simscape, Theor. Appl. Mech. Lett, Vol. 14, No.2, p. 100502, 2024.

[15] Sosa-Méndez, D., Lugo-González, E., Arias-Montiel, M. García-García, R. A.: ADAMS-MATLAB co-simulation for kinematics, dynamics, and control of the Stewart–Gough platform, Int. J. Adv. Robot. Syst, Vol. 14, pp. 1–10, 2017.

[16] Shi, G., Chen, S. Liang, G.: Analysis with ADAMS /ANSYS on Dynamic Properties of Rotating Hook - Lift Garbage Truck, in: *2009 International Confe–rence on Measuring Technology and Mechatronics Automation*, 2009, Huna, pp. 746–749.

[17] Delyová, I., Hroncová, D., Frankovský, P., Dzurišová, E. and Rákay, F.: Kinematic Analysis of Crank Rocker Mechanism Using MSC Adams/

View, Appl. Mech. Mater, Vol. 611, pp. 90–97, 2014.

[18] Hroncová, D., Frankovský, P., Virgala, I. and Delyová, I.: Kinematic Analysis of the Press Mechanism Using MSC Adams, Am. J. Mech. Eng, Vol. 2, No.7, pp. 312–315, 2014.

[19] Truc, L. N. and Lam, N. T.: Quasi-physical modeling of robot IRB 120 using Simscape Multibody for dynamic and control simulation, Turkish J. Electr. Eng. Comput. Sci, Vol. 28, pp. 1949–1964, 2020.

[20] Hong, T. D. and Thai, H. T.: Research and design of multi-directional dumping construction in trucks, Sci. J. Silesian Univ. Technol. Ser. Trans, Vol. 119, pp. 5–18, 2023.

[21] Jovanović, R., Bugarić, U. S., Vesović, M. V. and Perišić, N. B.: Fuzzy Controller Optimized by the African Vultures Algorithm for Trajectory Tracking of a Two–Link Gripping Mechanism, FME Trans, Vol. 50, No. 3, pp. 491–501, 2022.

[22] Nguyen, H. V., Cong, V. D. and Trung, P. X.: Development of a SCARA Robot Arm for Palletizing Applications Based on Computer Vision, FME Trans, Vol. 51, No. 4, pp. 541–549, 2023.

[23] Arian, A., Isaksson, M. and Gosselin, C.: Kinematic and dynamic analysis of a novel parallel kinematic Schönflies motion generator, Mech. Mach. Theory, Vol. 147, p. 103629, 2020.

NOMENCLATURE

a	acceleration (m/s^2)
B	damping coefficient (Ns/m)
C	leakage coefficient
D	pump displacment (m)
L	distance between points of link (m)
F	force at joint (N)
K	stiffness coefficient (N/m)
p	pressure (bar)
P	gravitational force (N)
Q	flow rate (Lpm)
M	mass of mechanism’s component (kg)
n	speed (rpm)
I	moment of inertia through the mass center (m^2)
r	distance form point to mass center (m)
S	cylinder area (m^2)
t	time (s)
V	cylinder volume (m^3)
x	piston position (m)

Greek symbols

α	Angular acceleration (rad/s^2)
ρ	Fluid density (kg/m^3)
φ	Angle between link and x-axis (rad)
v	cylinder velocity (m/s)
ω	Angular velocity (rad/s)

Subscripts

c	cylinder
m	mass center
n	nominal
o	atmospheric condition
p	pump

СТУДИЈА КИНЕТИКЕ И ДИНАМИКЕ МЕХАНИЗМА ЗА СТРУГАЊЕ-ПРИТИСКИВАЊЕ КОМПАКТОРА КАМИОНА ЗА СМЕЋЕ

М.К. Фам, Т.В, Ву, Л.К. Тран, Х.Х. Нгујен, Т.Д. Хонг

У овој студији је свеобухватно анализирана кинематика и динамика механизма за стругање-притискивање камиона за смеће коришћењем нумеричких метода. Вишетело интегрисано са хидрауличким симулационим моделом је успостављено да истражи рад механизма у складу са стварним радним условима у завршеном циклусу од 18 секунди. Модел је верификован прорачуном у стабилним временима, што је показало високу конзистентност. Резултати откривају да механизам ради у стабилном стању скоро све време, са брзинама цилиндра у распону од 0,08 до 0,15 м/с. Брзина и убрзање цилиндра снажно флуктуирају када механизам убрзава или успорава; међутим, ефекат инерције је безначајан. Силе које се приме–њују на спојеве су максималне на крају процеса пресовања. Занимљиво је да је сила која се приме–њује на спој који повезује стругање и клизну плочу највећа, три пута већа од споја између клизне плоче и цилиндра за пресовање и један и по пута већа од оне између плоче за стругање и цилиндра за стругање. Резултати студије могу се применити на процес пројектовања камиона за смеће у специ–јалним и специјализованим возилима уопште или се користити као референца за побољшање перфор–манси и оптимизацију масе, силе и материјала механизма.